FROST DILATION MEASUREMENTS ON CONCRETE CORES FROM A DAM WITH ASR

Stefan Jacobsen.[1,*], Jan Lindgård. [2] and Leonie Fritz [3]

[1]Norwegian University of Science and Technology, Departement Structural Engineering,
N-7491 TRONDHEIM, Norway

[2]SINTEF Byggforsk AS, Building and Infrastructure,
N-7465 TRONDHEIM, Norway

[3]École nationale des ponts et chaussées,
77455 MARNE LA VALLÉE, cedex 2, France

Abstract

In order to evaluate length change measurements to determine damage in concrete due to both ASR and internal frost attack, concrete cores drilled from a 25 year old dam with slight ASR and some surface frost damage were used. Critical dilation was measured during a single freezing and thawing cycle of moisture conditioned and -sealed specimens using LVDT and invar steel frame. The effects of varying degree of capillary saturation (DCS), pre-drying, specimen size and length of freezing period on unrestrained freezing dilation were studied. Critical freezing dilation testing is well suited to determine durability against internal frost damage. The existence of critical dilation, the deleterious effect of severe drying compared to the frost damage observed in specimens with mild drying and the mechanisms causing detectable frost damage were similar to what is found in the literature on laboratory cast concrete without ASR. The experiments also illustrate the useful information from the PF-method for determination of DCS and porosity including protective pore factor (PF). Critical dilation was found to be around 0.08 – 0.1 ‰ based on observations of freezing- and residual dilation on the 25 year old cores with DCS=92 – 100 %. Finally we propose a method of determining the interaction mechanism between ASR and frost damage based on the same criterion; namely strain.

Keywords: length change, frost dilation test, microscopy, moisture content, porosity, cracks

1 INTRODUCTION

The interaction between alkali silica reactions (ASR) and frost action is a likely cause of amplified degradation of concrete structures compared to when one of the two degrading mechanisms is acting alone. This paper, which is based on the experimental study [1] and an investigation of ASR in a Norwegian concrete dam, evaluates the use of freezing dilation testing to measure strains associated with frost damage in concrete with ASR.

The effect of simultaneous frost and alkali silica reaction (ASR) on deterioration of concrete structures has been addressed in very few studies compared to the amount of research performed on deterioration of concrete due to frost or ASR alone. In [2] testing was carried out on 3 ½ year old lab specimens affected by ASR before frost exposure. Freezing and thawing with water on the concrete surface gave higher expansion due to internal frost damage at a given degree of saturation compared to reference specimens with non-reactive aggregate. Thin section microscopy attributed the increased frost damage to pre-existing cracks with up to 0.3 mm width. Also ASR gel and other reaction products partly filling air voids were observed. Thus both cracks and reduced available air void protection may have amplified the effective water saturation. Similar acceleration of expansion due to combined frost and ASR was found in [3]. Generally, pre-existing cracks have been found to accelerate ASR expansion [4]. Therefore it appears that the sequence of events plays a role for the degradation. In [5] an experimental study of the effect of the sequence of events (first ASR then frost vs. first frost then ASR) showed that in both sequences the deterioration was accelerated compared to a reference case with only one type of damage. However, the relative effect of the two sequences of events could not be evaluated since frost degradation was measured as loss of relative dynamic modulus as function of number of cycles whereas ASR was measured as length increase as function of exposure time at elevated temperature and humidity. A recent proposal for ASR performance test [6] includes dry/wet-, warm/hot-, freeze/thaw cycles with varying salt solutions. It is capable of

* Correspondence to: stefan.jacobsen@ntnu.no

increasing the expansion. Unfortunately the degree of saturation, which is the main factor for frost damage, is not controlled in this test.

When evaluating the possibility of simultaneous ASR and internal frost damage it will be an advantage to use the same damage criterion and to control the degree of saturation. Expansion exceeding a certain strain is commonly used for evaluation of both frost- and ASR damage, even though the mechanisms leading to fracture are totally different. In order to proceed in the development of methods to determine the durability and service life of concrete structures with combined ASR and frost attack we have therefore assessed length change during freezing of concrete cores taken from a 25 year old dam with both ASR and slight surface frost damage (scaling). The objective is to evaluate the variation in strain due to internal frost attack, as degree of saturation, preconditioning, specimen size and frost attack varies.

2 TEST METHODS AND MEASUREMENTS

2.1 Strain due to ASR and internal frost attack

ASR laboratory tests of the reactivity of concrete and –constituents (aggregates, binders, concrete mix compositions) commonly measure expansion after specific curing and storage conditions as an acceptance/rejection criterion:

$$\varepsilon = \frac{l - l_0}{l_0} \qquad (1)$$

ε is residual strain or -expansion, l is length after a certain exposure and l_0 is length at start of test. ASR damage is caused by expansion beyond the concrete fracture tensile strain. In the Norwegian mortar bar method (submerged in 1 M NaOH at 80 ºC) for evaluation of reactivity of aggregate [7,8], similar to [9] maximum expansions of 0.8 – 1.4 ‰ are used. The maximum allowed expansion depends on the grading of the aggregate (coarse or fine). In the Norwegian concrete prism test (38 ºC and 100 % RH) [7] 0.4 – 0.5 ‰ maximum expansions are used. Expansion (in reality "crack intensity") due to ASR can also be estimated on structures by microscopy on fluorescence impregnated plane sections from cores [10], and by measuring widths of visually observed cracks on the concrete surface using surface crack index (SCI) [11]. Very limited experience exists from some Norwegian measurements on 50 – 60 year old dams with varying degrees of ASR and frost damage [12]. They showed expansion in the range 0.2 – 2 ‰ as average observed crack widths (taken as $(l-l_0)$) over the total traverse length (taken as l_0) according to [11] for several areas per dam.

In frost testing, strain is measured to characterize internal frost damage, or internal cracking due to frost. Also non-destructive measurements like increased ultra sonic pulse velocity and loss of resonance frequency [13, 14] are used. Internal frost damage is very clearly related to degree of saturation at freezing. Frost testing can therefore consist of measurement of a critical dilation due to freezing. It is done by adjusting and controlling the degree of saturation of a concrete specimen. Then the length change during one single freezing and thawing cycle is measured using Linear Variable Differential Transducers (LVDT) on a concrete specimen mounted in an invar steel frame . Figure 1 shows invar frames and figure 2 shows the two types of freezing cycles used. Damage occurring during freezing is observed as large expansion or freezing dilation deviating from the linear extrapolation of the pre-freezing contraction (which for concrete usually is $1.0 \cdot 10^{-5}$ °C^{-1}) measured during cooling [15-17] (figure 3). Such expansion during a single freezing and thawing cycle is called freezing dilation and the concrete fracture tensile strain (0.15 ‰) can be taken as damage criterion [15]. In repeated freeze/thaw cycle tests without control of the degree of saturation of the specimen, e.g. like [13, 14, 18, 19], the maximum allowed residual dilation (eq.(1)) after a specific number of freeze/thaw cycles is usually 1 ‰. The residual dilation in the critical dilation test (figure 3) should be registered as indication of permanent frost damage even though it is very low compared to in repeated freeze/thaw tests without control of the degree of saturation of the specimen during freezing [13, 14, 18, 19].

Frost damage also occurs as surface scaling. It is normally associated with freezing in the presence of deicer salt. The damage is usually measured as mass of scaled concrete [18] or characterized as fraction of damaged surface area by visual surface damage rating [19]. Both surface- and internal damage may of course be characterized in a test. Figure 4 shows scaling on a core from a horizontal surface.

In addition to the varying direct tests of strain due to ASR and internal frost damage some indirect microscopy-, porosity- and moisture content tests exist. For potential ASR the content of reactive rock types in the aggregate can be counted in a petrographic analysis [7], and for frost durability Protective pore Factor (PF)-test [20] and air void spacing factor [21] can be measured.

2.2 Measurements performed

A series of 100 mm diameter concrete cylinders were taken vertically from the top surface of the 25 year old Sandsavass dam using diamond coring. The specimens were identified by the local area on the dam (e.g. 1), core number (e.g. 3) in the area and depth (e.g. 0-200 mm); in this case 1-3/0-200. The cores were used for varying purposes in the survey of the condition of the dam [22]. Slight ASR was identified by microscopy on fluorescence impregnated plane- and thin sections. Cracks and gel were associated with greywacke [23]. In addition frost surface scaling could be seen to a depth in the order of a few mm, see figure 4. The specimens for microscopy, freezing dilation and strength were cut with diamond blade from the 100 mm diameter cores.

Some cores were moisture isolated in field immediately after sampling for measurement of moisture content and porosity. At the laboratory they were unpacked and 40 – 50 mm slices quickly cut off with a powerful sharp steel jaw, brushed, and their in-situ Degree of Capillary Saturation ($DCS_{in\text{-}situ}$) determined:

$$DCS_{in-situ} = \frac{w_{in-situ} - w_{105\circ C}}{w_{suc} - w_{105\circ C}} 100\% \quad (2)$$

$w_{in\text{-}situ}$ is weight of specimen with in-situ moisture content, $w_{105°C}$ is weight of specimens after 105 °C drying to constant weight and w_{suc} is weight after suction in water to constant weight. Specimens for frost testing were stored for some time at 50 % RH in lab-air before moisture conditioning. Their absorption after submersion in water ($w_{absorbed}$) for 2 – 6 weeks and their evaporable water contents (w_e) after being submerged, frost tested and dried at 105 °C to constant weight were determined. w_e obtained this way was 6.5 – 7.0 % of oven dry weight for the initially slightly air dried specimens and 6.3 – 6.5 % for the initially 105 °C dried specimens. The degree of capillary saturation after the storage for some time at 50 % RH in lab-air ($DCS_{lab\text{-}air}$) was calculated as follows:

$$DCS_{lab-air} = \frac{w_e - w_{absorbed}}{p_{suc} V \rho_{water}} 100\% \quad (3)$$

p_{suc} is given by eq.(4). The suction-(p_{suc}) and air void porosities (p_{air}) were determined using the PF-method [20]. Once-dried specimens were capillary saturated submerged and weighed giving $w_{cap\text{-}suc}$. Then the specimen volumes V were determined by weighing submerged and finally determining the pressure saturated weight $w_{pressure}$ after 24 hours in 10 MPa water pressure:

$$p_{suc} = \frac{w_{cap-suc} - w_{105\circ C}}{V \rho_{water}} \quad (4)$$

$$p_{air} = \frac{w_{pressure} - w_{cap-suc}}{V \rho_{water}} \quad (5)$$

These two porosities give the Pore protection Factor (PF) [20]:

$$PF = \frac{p_{air}}{p_{air} + p_{suc}} 100\% \quad (6)$$

In addition the degree of saturation (DS) expressing evaporable water content (w_e) as fraction of total porosity ($p_{suc}+p_{air}$) can be determined. This was done for specimens after frost testing, and using air- and suction porosities DCS and DS relate as:

$$DCS_{test} = \frac{w_e}{p_{suc} V} \text{ and } DS_{test} = \frac{w_e}{(p_{air} + p_{suc}) V} \text{ giving } DS_{test} = DCS_{test}(1 - PF) \quad (7)$$

Specimens for compressive strength testing were 172-188 mm long with test surfaces grinded parallel after sawing. Strength was measured after 3 days storage submerged in 20 °C water. Specimens for frost dilation testing were always 200 mm long. 8 mm diameter and 16 mm long invar studs were fixed by drilling 8 mm deep holes and gluing them with epoxy to the end surfaces of the cylinders. Then the specimens were moisture conditioned, moisture sealed and mounted in the invar frames in the freezer (figure 1), the LVDTs installed, set to zero and the specimen kept at 20 °C for some hours until constant length. Then the freeze/thaw cycles were started, see figure 2.

2.3 Frost test variables

The effects on freezing dilation of the following variables were studied:

Moisture state:

- Varying DCS after immersion to DCS=100% and air drying to mean DCS=97, 95 and 92%
- Dried at 105 °C to constant weight and saturated by immersion

Specimen size (slightly dried and saturated to DCS=100%):

- 1/1 cylinders Ø=100 mm, L=200 mm
- ½ cylinders (cut along length axis), L=200 mm
- ¼ cylinders (cut along length axis, see photo in figure 1), L=200 mm

Prolonged freezing period (slightly dried and saturated to DCS=100%):

- 3 hours at minimum temperature
- Prolonged freezing period; 24 hours at minimum temperature

Specimens to be frost tested at DCS < 100 % were slightly air dried from DCS=100 % to 97, 95 and 92 %, respectively. A quite homogeneous moisture distribution was expected since the cores for frost dilation testing were slightly air dried in the lab to DCS of 53 - 73 % before being immersed (table 2). Due to the gradient of moisture over the 100 mm diameter of the slightly dried cylinders the immersion should mostly fill pores near the surface. The subsequent slight drying thus contributed to a more homogeneous moisture distribution for specimens with target DCS < 100 %. The 105 ºC drying was chosen to increase the ice formation [24, 25] and to observe the expected increase in freezing dilation due to a coarser and more continuous pore system [25]. The effect of reduced specimen size was tested at DCS=100 % to be compared with the large cores with 100 mm diameter. A prolonged freezing period was tested at DCS=100 % to observe any effect on expansion of time dependant ice formation.

3 RESULTS

Strength, porosity and moisture content

Table 1 shows strength, porosities and PF of the concrete and in-situ saturation. Table 2 shows moisture content in the frost tested specimens and DCS after drying in lab-air before saturation and frost testing. Figure 2 shows concrete surface temperature vs. time during freezing and thawing. An air cooled freezing cabinet was used between + 20 and -18 °C at approximately 8 °C/h cooling rate.

Effect of varying DCS by saturation from slightly air dried state

Figures 3 and 5 show concrete surface temperature versus strain during freezing and thawing for specimens re-saturated from lab-air dried condition to DCS 100, 97, 95 and 92 % and frozen once.

Effect of re-saturation after severe drying at 105 °C

Figure 6 shows the effect of severe pre-drying at 105 °C before re-saturation and freezing with length measurements.

Effect of specimen size

Figure 7 shows the effect of specimen size at freezing of a half and a quarter section of 200 mm long concrete cores, both sawn parallel to their length axes before saturation to DCS=100 %.

Effect of prolonged freezing period

Figure 8 shows the two specimens saturated to DCS=100 % and frozen with the 24 hour prolonged freezing period shown to the right of figure 2.

4. DISCUSSION

4.1 Concrete quality and effect of moisture state

Table 1 shows that the air void content in the two areas giving mean PF=17 and 22 % is on or a bit lower than the recommended air content. The quality of the concrete is also a bit poor with respect to freezing with fresh water. [20, 26] recommend w/c < 0.40 – 0.45, whereas w/c in this dam was estimated at 0.65 – 0.75 in [22, 23] in line with the low strength of 31-34 MPa. The recommended PF > 20 % is thus not fulfilled for area 1. The cores were taken from horizontal surfaces exposed to the weather in the mountains of south central Norway. The rather high DCS observed in situ, 93.5 –

97 %, is in line with earlier measurements in similarly exposed concrete foundations and dams in Norway [27, 28].

Figure 3 shows that the freezing dilation in the most saturated specimen to the left (100 % DCS) causes a much larger freezing dilation and residual expansion compared to the specimen to the right. Also the dilation of the specimens in figure 5 with DCS ≤ 97 % shows no residual expansion after melting. This indicates that the deviation of the two parallel freezing and thawing curves at DCS=100 % can be attributed to permanent damage. The temperature lag effects between the freezing and melting curves causing different strain distribution over the cross section during freezing and cooling should be equal for specimens with and without damage. Based on residual expansion it thus seems from the experiments that the critical dilation is somewhere between 0.14 and 0.08 ‰ for these slightly ASR- and surface frost deteriorated concretes. Note that the figures also show that contraction occurs during freezing. For the highly saturated specimens this is most clearly seen before ice formations increases too much; at around -3 to -7 ºC during freezing in figure 3. For the presumably less than critically saturated specimen to the right in figure 5 contraction or shrinkage is seen all the way to the minimum temperature. This is in line with the observations [29-32].

Note that different specimens with equal DCS had rather large differences in max dilation. The parallel specimen to 1-3/0-200 in figure 3; 1-3/200-400 (not shown, DCS=100 %) had only half the freezing dilation; 0.7 ‰ max dilation at -13 ºC (but similar residual expansion as 1-3/0-200). There are at least five factors that could explain the different behavior between freezing and melting. One is variation in the onset of the initial ice formation which can vary somewhat between samples due to the spontaneous nature of the first ice nucleation and its consequences for propagation of ice through the pore system [24, 25, 29, 30, and 33]. Another reason could be differences in concrete quality, for example between surface and inner part from the production, or some kind of ageing of the concrete. A third reason could be internal differences in degree of saturation (DS) due to variations in air void content. DS may then vary more than DCS according to eq.(5) and (7) due to individual variations of PF in the cores as can be seen in table 1. A fourth reason is the hysteresis between freezing and melting of pore water [24, 25, and 30]. A fifth possible reason is of course differences in the LVDTs.

Figure 6 shows that the severe 105 °C drying before re-saturation gave large freezing dilation of 0.23 and 0.48 ‰, respectively. The freezing clearly has resulted in frost damage in terms of residual length change. The change in shape of the curves of the 105 ºC dried and re-saturated specimens is quite dramatic with a rather steep freezing dilation compared to what has been seen before, and melting at higher temperature compared to the mildly air dried specimens. The reason is the finer pore structure of the mildly air dried concrete specimens where the phase change takes place at lower temperature compared to the 105 °C dried specimens. In the latter specimens the coarse pore structure makes most of the water melt closer to zero. The large freezing dilation commences without the initial contraction seen in several cores that had only been air dried before re-saturation. Also it appears that the permanent damage is larger than in the most highly saturated specimens without the severe pre-drying. As discussed above, it seems that the residual dilation, or difference between the cooling and heating part of the cycle is thus mainly caused by permanent damage to the concrete.

4.2 Effect of specimen cross section size

Figure 7 shows freezing dilations of rather thin specimens with 25 and 50 % of the cross sectional area made by gutting the cores along the length axis into halves or quarters. All lengths were 200 mm. The specimens had DCS=100 % and can therefore be compared with the DCS=100 % specimen in figure 3. There seems to be no clear effect of cross sectional size at DCS=100 % since the dilation of the quarter cylinder (1/4 in figure 7) is similar to the largest dilation measured on big cylinders at DCS=100 % (figure 3). The cylinder with half cross section (1/2 in figure 7) has similar dilation as the lowest dilation measured on big cylinders at DCS=100 % (figure 3). Also an interpretation of the lag between the cooling and the melting curves as permanent damage is supported since the permanent damage seems to be similar in the small specimens with rather equal DCS.

4.3 Effect of length of freezing period

Figure 8 shows that more contraction occurs while the specimens are kept an extra 24 hours at the minimum temperature compared to the specimen with DCS=100 % of figure 3 with the short (ordinary) freezing cycle (see figure 2). The explanation is probably the kind of ice lens growth discussed in the cement paste experiments of Helmuth [29, 30]. A permanent frost damage in terms of residual length change of approximately 0.04 ‰ follows the freezing dilation of 0.07 – 0.1 ‰. That is, the damage caused by the freezing dilation, presumably due to some kind of hydraulic pressure during

the primary ice formation, is irreversible. It cannot be "closed" again by the contraction or shrinkage caused by the ice formed during prolonged constant minimum temperature.

The expansion during cooling and the subsequent contraction at constant minimum temperature also point to some kind of protective effect by the pore system during continued and slower ice formation compared to the expansion during primary ice formation. One possible consequence of this that remains to be proven is whether this concrete at a sufficiently low cooling rate could be frost durable at this DCS.

4.4 Various observations

From the pre-freezing contraction part of the cooling curves we see that the thermal contraction of the concrete is around 10^{-5} ºC. As a whole the study confirms that the freezing dilation measurements were able to detect frost damage on the slightly ASR damaged cores, and with similar effects to what is reported in the literature on laboratory cast concrete without ASR. These effects are the existence of critical dilation, the deleterious effect of severe drying compared to the frost damage observed in specimens with mild drying and the two frost damage mechanisms causing detectable length change; 1) large expansion due to hydraulic type pressure exerted by propagating ice [30, 34] and/or flowing water due to the expansion of the primary ice formation along with 2) ice lens formation [29, 30]. The ice lens formation gave some initial shrinkage before critical expansion (figure 3) or only shrinkage in less than critically saturated concrete (figure 5) as well as continued growth of ice lenses at prolonged storage at minimum temperature causing shrinkage at minimum temperature (figure 8). The observations of initial shrinkage or only shrinkage at freezing and during prolonged freezing are in line with Helmuths observations on cement paste. The initial shrinkage before the critical expansion in highly saturated specimens confirms that 1) and 2) occur simultaneously.

The freezing dilation behavior of concrete cores taken from dams with slight surface frost scaling and ASR damage is similar to what has been observed earlier on different laboratory cast specimens [15, 26, 29-32]. The critical DCS as strain exceeds 0.15 ‰ at freezing seems to be quite high; near 100 % for the present concrete. Specimens dried at 105 ºC before re-saturation and frost exposure seem to be damaged at lower water saturation due to the amplified freezing dilation shown in figure 6.

The critical DS is somewhat lower than the critical DCS=97 % observed in these experiments according to eq.(7) and using the PF of table 1: critical DS=97 (1-0.17)=80.5. This agrees with the frost durability criterion PF > 20 %. Based on the permanent damage in the form of permanent length change seen on specimens frozen with DCS=100 % as well as the slight surface frost damage observed on the dam, it seems that the concrete in the dam is not frost durable when exposed to freezing after wet periods longer than a few weeks. Also the compressive strength is a bit low as already discussed.

A possible hypothesis for interaction between frost attack and ASR could be that either frost damage may give cracks that are further developed by ASR or that ASR may accelerate internal frost attack. However, whatever sequence of events we recommend that evaluation of the frost component in degradation due to combined ASR and frost action is evaluated with freezing dilation measurements and related to the ASR expansion. A critical freezing dilation around 0.08 – 0.1 ‰ should be used, and residual dilation > approximately 0.02 – 0.04 ‰ is an indication of permanent frost damage. Two test series should therefore be set up: 1) ASR testing of specimens that initially have experienced one freezing cycle at three different levels of DCS giving them less than critical dilation, critical dilation and larger than critical dilation, respectively. 2) Frost dilation testing of specimens that initially have experienced ASR expansion well below, at and above the acceptance criteria for ASR expansion. Enough specimens must be made so that frost dilation testing can be performed at different DCS giving expected less than, at and above critical DCS. In all cases length change measurements are used to quantify the damage.

One could also investigate whether ASR affected specimens generally produce fewer and wider cracks than specimens deteriorated by frost by performing microscopy after the different tests. Also the significance of the surface ageing could be tested as freezing dilation normal to the core length axis near the surface and deeper into the concrete. Furthermore one could perhaps also use the mixes and specimens for evaluation of ASR-reactivity of different aggregates [7-9] for frost dilation testing to evaluate the two forms of degradation with equal damage criteria. Finally the significance of the in-situ moisture contents of table 1 for in-situ freezing dilation should be measured. Measurements have been made [35] indicating that in-situ ice formation in a Swiss bridge was much slower and with less super cooling than in laboratory tests. In addition there is the effect of restrain in-situ which should reduce the expansion compared to the free expansion of our relatively small specimens.

5 CONCLUSIONS

Freezing dilation/strain measured during freezing of concrete specimens from a dam with slight ASR and frost damage show that the test is well suited to determine durability against internal frost damage. The existence of critical dilation, the deleterious effect of severe drying compared to the frost damage observed in specimens with mild drying and the two frost mechanisms causing detectable length change were similar to what is found in the literature on laboratory cast concrete without ASR. The experiments also illustrate the very useful information from the PF-method for determination of DCS and porosity including protective pore factor (PF). Critical dilation was found to be around 0.08 – 0.1 ‰ based on observations of residual dilation in a series of concrete specimens with DCS=92 – 100 %. We recommend that further investigations on combined ASR and frost action use strain as damage criterion by exposing specimens with varying ASR expansion to frost dilation testing at different DCS and measuring ASR expansion in specimens with varying residual expansion after freezing at varying DCS.

6 REFERENCES

[1] Fritz L. (2006): Measurements of length change during freezing of concrete with variable parameters, project work. Norwegian University of Science and Technology, Department of Structural Engineering: pp71 + 7 app.

[2] Trägårdh, J, Lagerblad, B (1996): Influence of ASR expansion on the frost damage of concrete, Proc. Nordic seminar Frost resistance of building materials, Ed.: S. Lindmark, Univ of Lund, Sweden Report TVBM-3072: pp 111-119.

[3] Bérubé M.A., Chouinard D., Boisvert L., Frenette J., Pigeon M. (1996): Influence of wetting-drying and freezing-thawing cycles, and effectiveness of sealers on ASR, Proc. 10th Int conf AAR in Concrete, Melbourne Australia: pp 1056-1063.

[4] Jacobsen S., Marchand J., Gérard B. (1998): Concrete Cracks I: Durability and self healing – a review, Proc Consec 98 V.1 Ed.Gjørv, Sakai, Banthia, E&FN Spon, London pp 217-231

[5] Sun W., Zhan B., Sha J. (2005): Experimental investigation of damage in concrete under combined effect of freeze-thaw cycles and ASR, Proc. Conmat, Vancouver, Canada: pp11.

[6] Stark, J, Giebson, C, and Seyfarth, K (2006): Personal communication and presentation RILEM TC-ACS.

[7] Norwegian Concrete Association (2005): Publication no. 32, Alkali aggregate reactions in concrete. Test methods and requirements to laboratories, Oslo 29 p. (In Norwegian)

[8] Norwegian Concrete Association, NB (2004): Durable concrete containing alkali reactive aggregates. NB Publication No. 21:2004 (in Norwegian): 22+12 pages including appendices

[9] RILEM (2000): AAR-2 - Detection of potential alkali-reactivity of aggregates - the ultra-accelerated mortar bar test. Materials & Structures (33): pp 283-289.

[10] Lindgård, J., Haugen, M., Skjølsvold, O., Hagelia, P. and Wigum, B.J. (2004): Experience from evaluation of degree of damage in fluorescent impregnated plane polished sections of half-cores based on the "Crack Index Method", paper pres at 12th ICAAR Conference, Beijing: pp. 939-947.

[11] Laboratoire des ponts et chausses (1997): Method d'essai no 47, Determination de l'indice de fissuration d'un parament de béton, Paris (In French)

[12] Birkeland B.A. (2006): Condition change of concrete dams due to alkali-aggregate reactions, M.Sc, Norw Univ of Science and Tech, Dept of structural engineering 59 p + 8 app. (In Norwegian)

[13] ASTM C666 (1987): Standard test method for resistance of concrete to rapid freezing and thawing, Annual Book of ASTM Standards 04.02, pp 410-417

[14] Tang, L, and Petersson, PE (2004): Freeze/thaw resistance of concrete – internal deterioration, Final recommendation test method RILEM TC 176-IDC, Materials and Structures Vol.37 pp 754-759

[15] ASTM C671 (1987): Standard test method for critical dilation of concrete specimens subjected to freezing, Annual Book of ASTM Standards 04.02 pp 427-433

[16] Fagerlund G. (1977): The critical degree of saturation method of assessing the freeze/thaw resistance of concrete, Materials and Structures no.10 pp 217-229

[17] SP method 2280 (1996): Critical dilation test of concrete specimens subjected to freezing – a modified method of ASTM C671 with the Øresund requirements amendments 11 p.

[18] Swedish Standard SS137244 (2005): Concrete testing – hardened concrete – scaling at freezing, 4th ed, Swedish Standards Institute ICS 91.100.30

[19] ASTM C672 Standard test method for scaling resistance of concrete surfaces exposed to deicing chemicals, Annual Book of ASTM Standards 04.02 (1987) 434-436
[20] Sellevold E.J. and Farstad T. (2005): The PF-method – A simple way to estimate the w/c-ratio and air content of hardened concrete. In: Proceedings of ConMat'05 and Mindess Symposium. Vancouver, Canada: The University of British Colombia. ISBN 0-88865-810-0., 10 p.
[21] ASTM C457 (1987): Standard test for microscopical determination of air void content and parameters of the air void system in hardened concrete, Annual Book ASTM Std 04.02 292-307
[22] Birkeland B.A., Alkali aggregate reactions in concrete dams, project work, Norw Univ of Science and Tech, Dept of structural engineering (2006) 43 p.+7 app. (In Norwegian)
[23] Haugen M., Lindgård J., Laboratory investigations of concrete cores from the Sandsavass dam, Sintef Concrete Dept., Test report 80113 (2005) 14 p
[24] Bager D.H, Sellevold E.J., Ice formation in hardened cement paste – II. Steam-cured pastes with variable moisture contents, Durab.build mat, ASTM STP 691 Sereda-Litvan Eds. (1980) 439-454
[25] Bager D.H, Sellevold E.J., Cement and Concrete Research V.16 (1986) 835-844
[26] Vuorinen J., On the behaviour of hardened concrete during freezing, VTT publ. 145 (1969) 148 p.
[27] Rodum E., Lindgård J., Skjølsvold O., Sellevold E.J., Gundersen H. (2001): Repair of frost damaged concrete foundations exposed to severe climate. In: Banthia N., Sakai K. and Gjørv O.E., Concrete Under Severe Conditions, Vancouver Canada: pp 2079-2087.
[28] Lindgård J., Rodum E., Pedersen B. (2006): Alkali-Silica Reactions in Concrete – Relationship between water content and observed damage on structures. In: Malhotra V.M., 7th CANMET/ACI int. conf. on Durability of concrete, Montreal: pp 147-165.
[29] Powers T.C., Helmuth R.A. (1953): Theory of volume changes in hardened portland cement paste during freezing, Proc Ann. Meet Highw Res Board V.32, Wash. DC pp 285-297
[30] Helmuth R.A., Capillary size restrictions on ice formation in hardened Portland cement pastes, Proc 4th Int Symp. Chemistry of Cement Vol.II, Nat. Bur of Standards (1960) 855-869
[31] Fridh K., Internal frost damage in concrete – experimental study of destruction mechanisms, University of Lund, LTH, Sweden, Report TVBM-1023 (2005) 276 p + 5 app.
[32] Jacobsen S., Bager D.H., Kukko H., Luping T., Nordström K. (1999): Measurement of internal cracking as dilation in the SS 137244 frost test, Project rep 250, Norw Build Res Inst. 26 p+5 app
[33] Defay R., Prigogine I., Bellemans A., Everett D.H. (1966): Surface tension and adsorption, Longmans, London (1966) 432 p.
[34] Powers T.C. (1949): The air requirement of frost resistant concrete, Proc Ann. Meeting Highway Research Board V.29, Washington DC pp 184-211
[35] Kaufmann J. (1999): Experimental identification of damage mechanisms in cem. por. materials on phase transition of pore solution under frost deicing salt attack, PhD thesis No 2037, EPFL 193 p.

Table 1: Compressive strength, porosities, PF and in-situ saturation

Specimen	Comp str (MPa)	p_{suc} (vol-%)	p_{air} (vol-%)	PF (%)	$DCS_{in-situ}$ (%)
1-2	31.2				
1-4/0-45		15.5	3.8	19.7	95.2
1-4/45-90		17.3	3.4	16.4	94.0
1-4/90-135		17.4	3.4	16.3	93.6
1-4/400-440		15.2	2.9	16.0	96.5
2-1/0-50		14.0	4.6	24.7	96.9
2-1/50-100		13.9	3.9	21.9	96.3
2-1/350-400		14.0	3.5	20.0	95.7
2-4	34.3				

Table 2: Saturation at frost testing and at air drying before saturation

Test	Specimen	$DCS_{lab\text{-}air}$ (vol%)	DCS_{test} (vol%)	W_e (weight%)
Varying DCS	1-3/0-200	54	100	7.0
	1-3/200-400	57	100	6.9
	1-5/0-200	53	97	
	1-5/200-400	61	95&92	
Dried at 105°C before suction	2-4/0-200	61*	100	6.3
	1-4/140-340	53*	100	6.5
Specimen size	1-1/200-400(1/2)	71	100	6.8
	1-1/200-400(1/4)	73	100	6.5
Prolonged freezing	1-6/0-200	58	100	6.9
	1-6/200-400	59	100	6.9

*: air drying before drying at 105 ºC

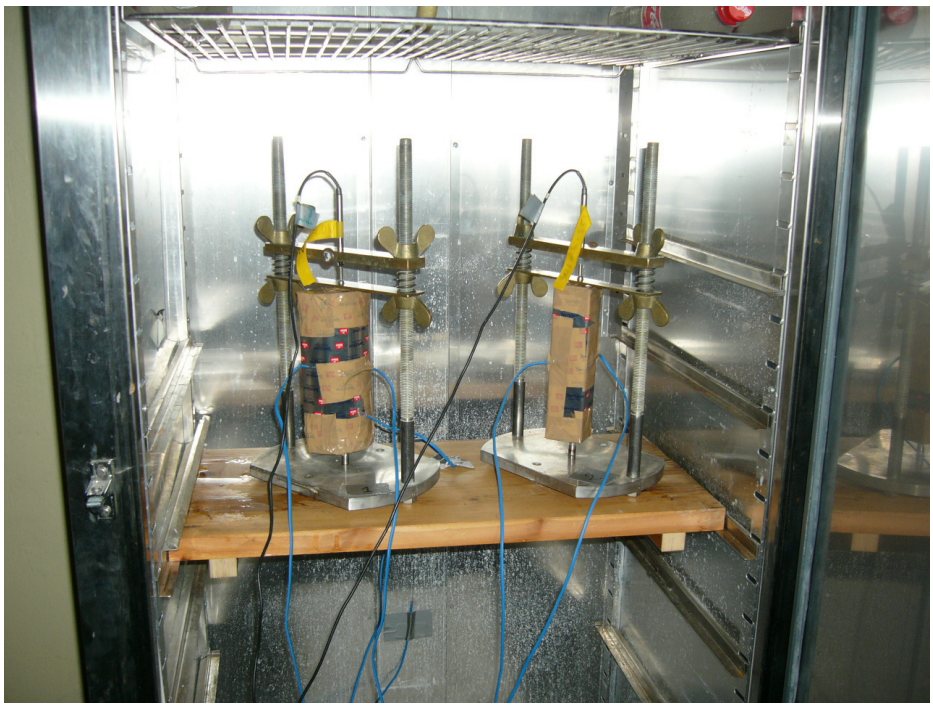

Fig. 1: Invar steel frames with LVDTs and moisture sealed specimens in freezer, left: 1/1 (Ø100/h200 mm), right: ¼ (radius 50/h200 mm)

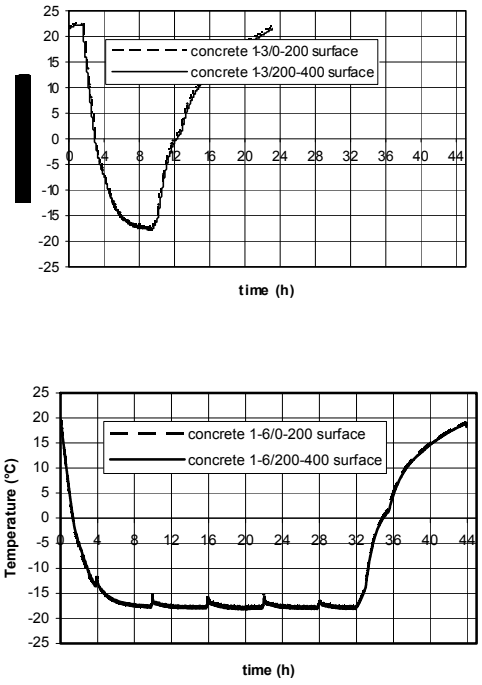

Fig.2: Concrete surface temperature vs. time; 3 h min. temperature (left) vs. 24 h prolonged freezing (right)

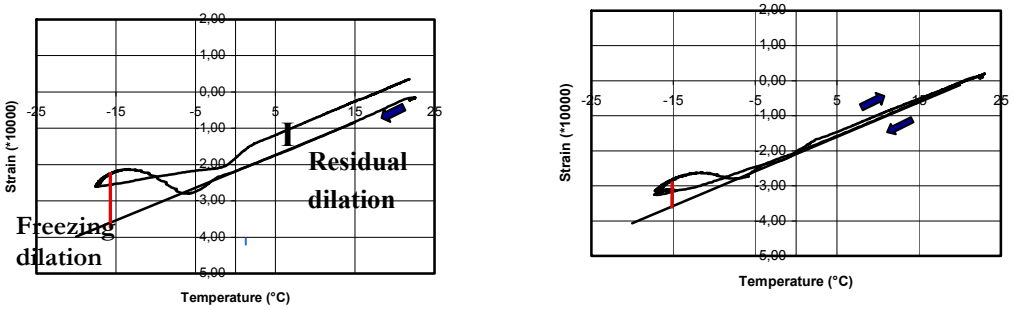

Fig.3: Freezing dilation of specimen 1-3/0-200 at DCS=100% with max dilation 0.14 ‰ at -16 °C (left) and 1-5/0-200 at DCS=97 % with max dilation 0.08 ‰ at -15 °C (right)

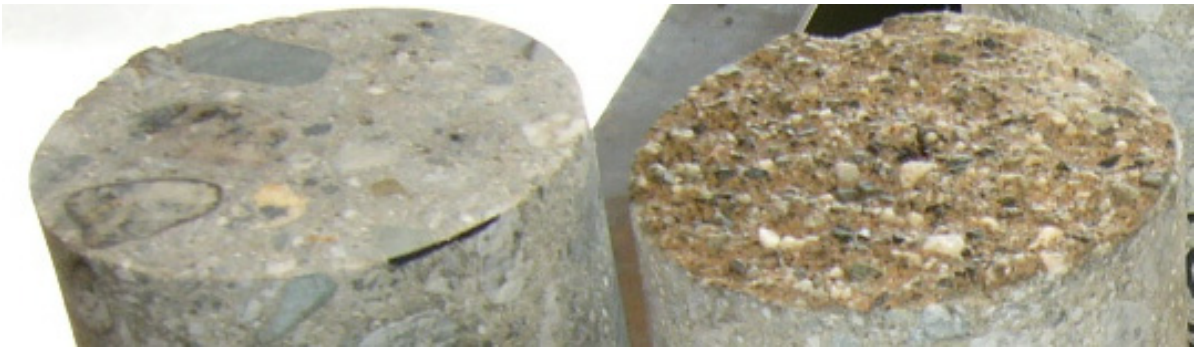

Fig.4: 100 mm diameter cores; left: sawn surface, right: horizontal dam surface with real frost scaling

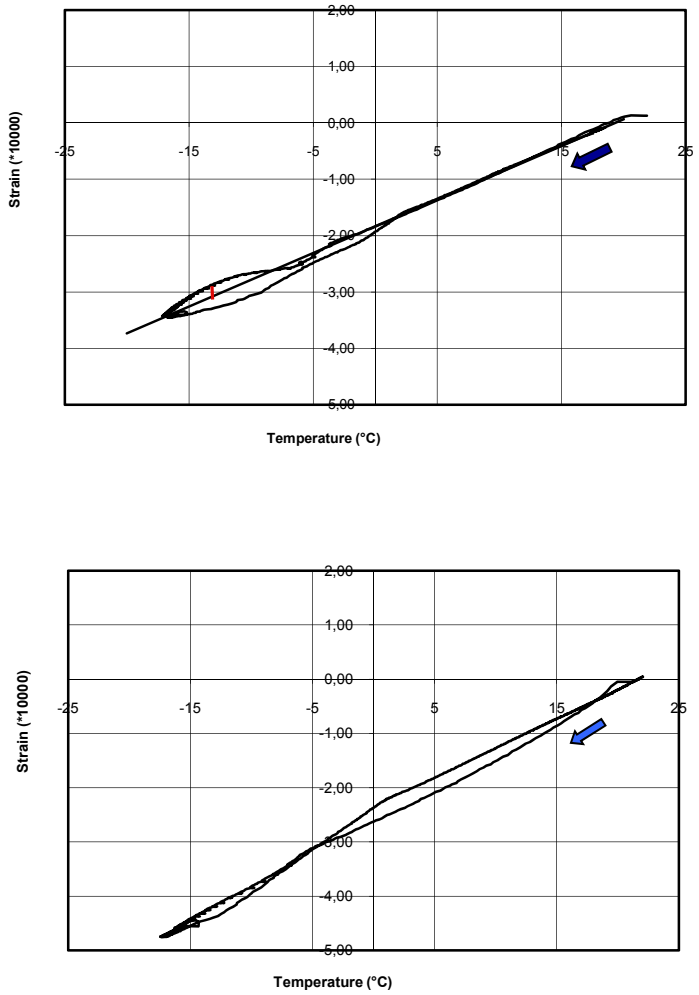

Fig. 5: Freezing dilation of specimen 1-5/200-400 at DCS=95% with max dilation 0.02 ‰ at -13 ºC (left) and the same specimen further dried to DCS=92 % and re-tested giving slight contraction (right)

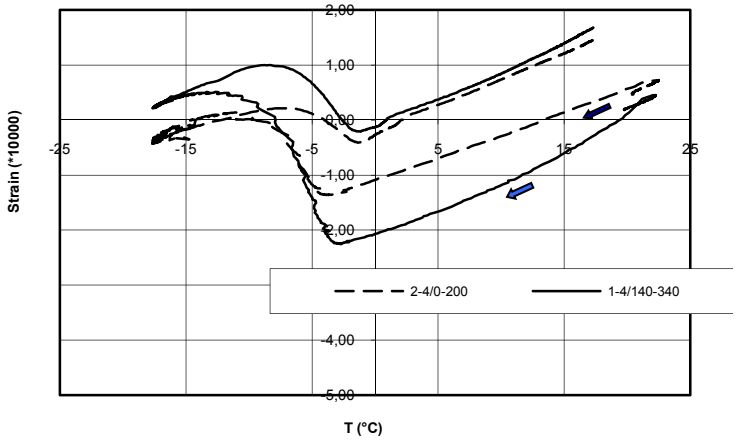

Fig. 6: Freezing dilation of specimen 2-4/0-200 and 1-4/140-340 after severe pre-drying with max dilation 0.23 ‰ at -14.5 ºC and 0.48 ‰ at -14 ºC, respectively

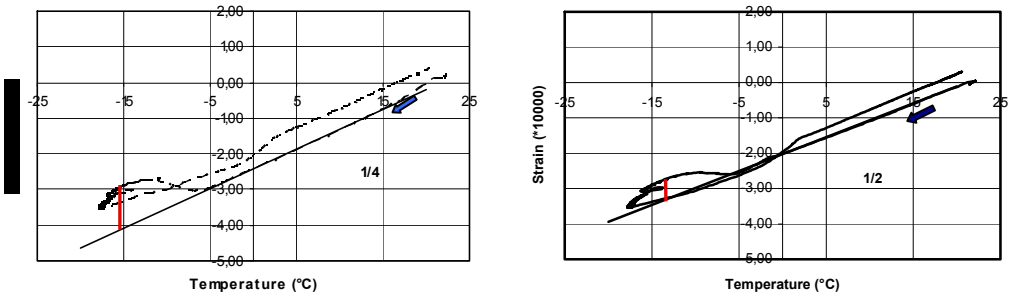

Fig. 7: Freezing dilation of specimens with different size; 1-1/200-400 (1/4): max dilation 0.12 ‰ at -16 °C (left) and 1-1/200-400 (1/2): max dilation 0.06 ‰ at -13 °C (right), both with DCS=100 %

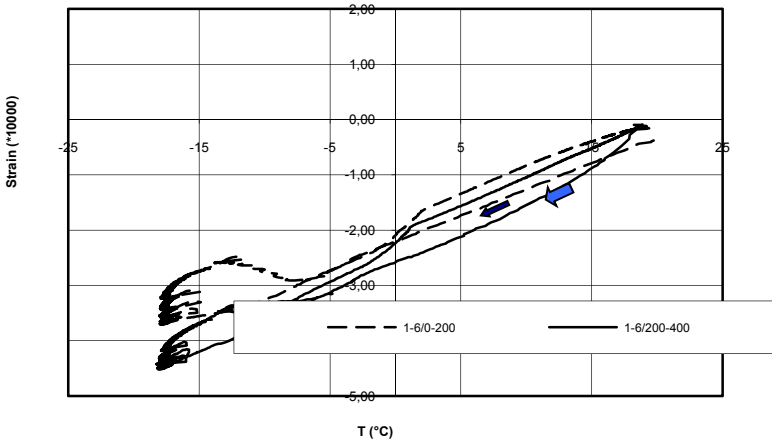

Fig. 8: Prolonged freezing period of specimen 1-6/0-200 and 1-6/200-400 at DCS=100 % with max dilation 0.1 and 0.07 ‰, respectively.